Resolving subsurface structure from cross-correlations of continuously recorded ambient noise at Long Beach, CA

Jason P. Chang, Taylor Dahlke, Nori Nakata, and Biondo Biondi
Department of Geophysics, Stanford University

BACKGROUND AND MOTIVATION

Identifying subsurface structures is vital to a number of fields, including earthquake hazard analysis and groundwater monitoring. Active-source seismic surveys are effective at resolving these types of structures, but they are often expensive and disruptive. As seismic arrays become larger, denser, and longer-duration, an increasingly viable alternative to active-source surveys is to extract coherent seismic signal hidden in continuous recordings of Earth's ambient seismic field. Here, we transform massive quantities of seismic noise data into coherent signal using cross-correlation techniques. We then use these seismic signals to resolve subsurface structures beneath Long Beach, CA.

AMBIENT NOISE CROSS-CORRELATION (ANCC)

ANCC aims to generate virtual sources by correlation of seismic noise recordings (Claerbout, 1968; Wapenaar, 2004). The seismic signal C between two receivers x_A and x_B is obtained by applying the following cross-correlation equation to their continuous noise recordings U in the frequency domain:

$$C(x_B, x_A, \omega) = \left\langle \left(\frac{U(x_B,\omega)}{|U(x_B,\omega)|} \right) \left(\frac{U^*(x_A,\omega)}{|U(x_A,\omega)|} \right) \right\rangle$$

where ω is frequency, * is the complex conjugate, |•| is the real absolute value of the spectrum, and <•> is the time-averaged ensemble (Bensen et al., 2007). The quality of the signal improves as more recordings are used. This formula recovers both waves that travel along the surface (surface waves) and waves that travel through the subsurface (body waves). Figure 1 illustrates our cross-correlation workflow.

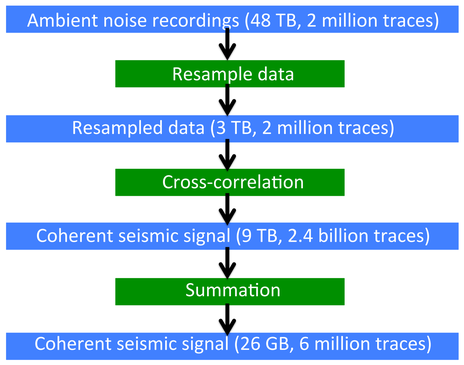

Figure 1: Flow chart of cross-correlation processing steps. From 48 TB of data, we synthesize 26 GB of coherent seismic data.

LONG BEACH SEISMIC ARRAY

- 8.5 x 4 km^2 region
- 2400 vertical-component geophones
- 100 m average station spacing
- 3 months of continuous (24 hr/day) recordings
- 2 ms sampling rate

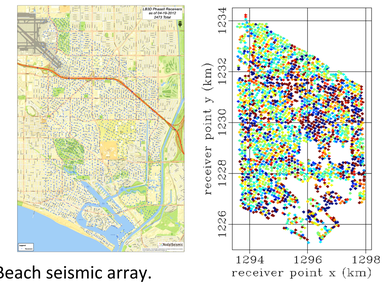

Figure 2: Left: Map of the Long Beach seismic array. Right: Snapshot in time of recorded ambient noise.

REFERENCES

Benson, G., M. Ritzwoller, M. Barmin, A. Levshin., F. Lin, M. Moschetti, N. Shapiro, and Y. Yang, 2007, Processing seismic ambient noise data to obtain reliable broadband surface wave dispersion measurements: Geophysical Journal International, **169,** 1239-1260.

Claerbout, J.F., 1968, Synthesis of a layered medium from its acoustic transmission response: Geophysics, **33**, 264-269.

Lawrence, J. F., 2014, Improved seismic ambient noise analyses with the adaptive covariance filter: J. Geophys. Res. (in review).

Wapenaar, K., 2004, Retrieving the elastodynamic Green's function of an arbitrary inhomogeneous medium by cross correlation: Physical Review Letters, **93**, 254301.

ESTIMATED SURFACE WAVES

By cross-correlating the recordings at one receiver with all other receivers in the array, we transform that receiver into a virtual seismic source. The seismic signals emitted by these virtual sources are typically dominated by surface waves (Figure 3).

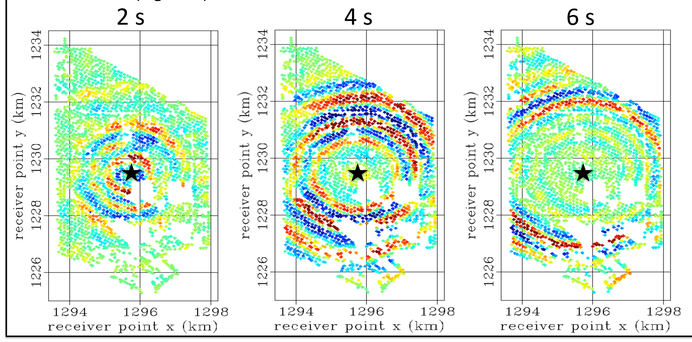

Figure 3: Snapshots in time of a virtual-source gather (0.75-1.25 Hz) in map view for a source in the center of the array (indicated by the star). Left: 2 s. Middle: 4 s. Right: 6 s. The strong wavefronts propagating away from the virtual source are surface waves. Results are derived from 35 days of data.

ESTIMATED BODY WAVES

To detect body waves, we focus on higher frequencies (3-15 Hz) and sum over all virtual-source gathers (Figure 4). We implement the following post-correlation processing steps to extract diving body-wave energy from individual receiver pairs (Figures 5 and 6).

1) Apply Gaussian-shaped taper to each correlation result to set signal outside of expected body-wave arrival time to zero

2) Compute correlation coefficient between each correlation result and the corresponding trace in the super-source gather (Figure 4)

3) Accept only correlation results with a correlation coefficient above 0.3 (retains 10% of data)

4) Apply adaptive covariance filter (ACF) to suppress incoherent energy in each correlation (Lawrence, 2014)

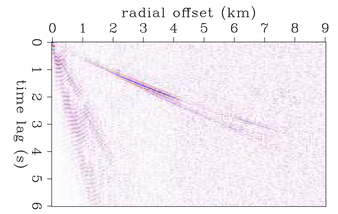

Figure 4: Virtual super-source gather after summing over all cross-correlation results (3-15 Hz). Body waves are now apparent.

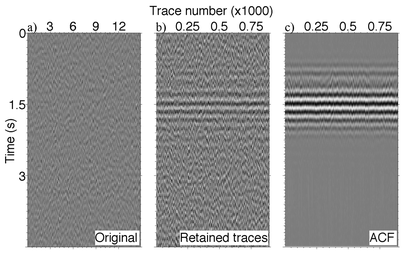

Figure 5: Correlation results at one radial offset throughout the post-correlation processing procedure. (a) original correlations. (b) retained correlations after applying correlation coefficient filter. (c) correlations after ACF.

Figure 6: Snapshots in time of a virtual-source gather (3-15 Hz) in map view for a source in northern part of the array (indicated by cross). The strong wavefronts propagating away from the virtual source are body waves. Blue line represents wavefronts with velocity 2.0 km/s.

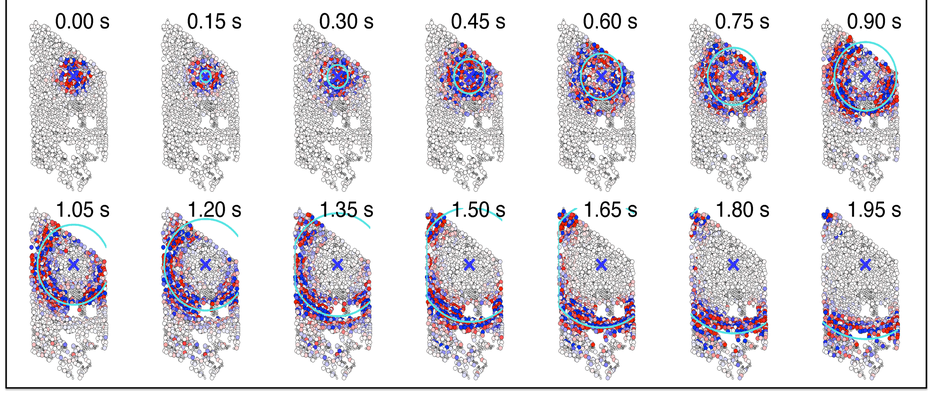

ACKNOWLEDGMENTS

We would like to thank Signal Hill Petroleum, Inc. for access to the data set and permission to publish. We would also like to thank Greg Beroza, Bob Clapp, Dan Hollis, Jesse Lawrence, Stew Levin, and Sjoerd de Ridder for helpful discussions and their help handling the data. Many thanks to the sponsors of Stanford Exploration Project for their financial support.

SURFACE-WAVE TOMOGRAPHY

By turning each receiver into a virtual source, we can generate a full virtual seismic survey. The arrival time of these surface waves are used for surface-wave eikonal tomography on a model domain discretized by Delaunay triangles. The high-velocity region in the southern part of the array coincides with the Newport-Inglewood fault (Figure 7).

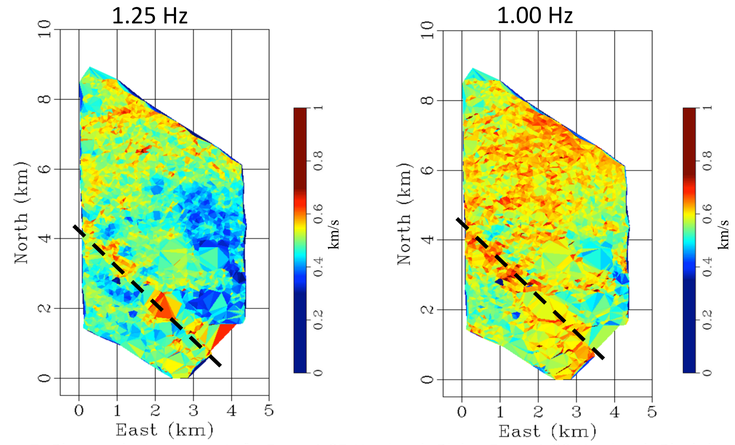

Figure 7: Phase-velocity maps. Left: From 1.25-Hz signal. Right: From 1.00-Hz signal. Black lines indicate the Newport-Inglewood fault. Lower frequencies are sensitive to deeper depths.

BODY-WAVE TOMOGRAPHY

By using body waves in a tomographic workflow, we obtain higher-resolution subsurface structures compared to those obtained from surface-wave tomography. The high-velocity zone in the southern part of Figure 8 suggests the presence of the Newport-Inglewood fault.

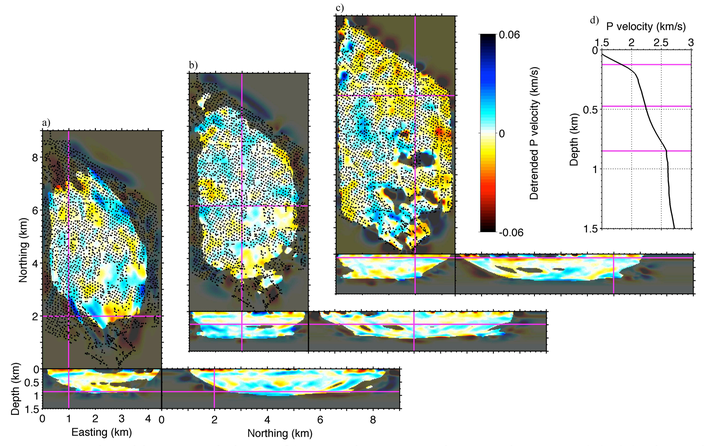

Figure 8: Vertical and horizontal slices of inverted P-wave velocity cube. From (a)--(c), slices shift shallower, east, and north. Purple lines show the location of slices. Velocities are detrended by subtracting the horizontally averaged one-dimensional velocities shown in panel (d). The colormap is valid for panels (a)-(c), where blue indicates faster velocities than the velocity in panel (d). The shaded areas in the velocity slices are poor ray coverage areas.

CONCLUSIONS

- Cross-correlation of 48 TB of continuous ambient seismic noise recordings at Long Beach, CA extracts 26 GB of coherent seismic
- Surface-wave tomography for different frequencies reveals a high-velocity region that coincides with the Newport-Inglewood fault
- Post-correlation processing (correlation coefficient filtering, adaptive covariance filter) enhances body-wave energy between individual receiver pairs
- Body-wave tomography provides a high-resolution velocity model that also resolves a high-velocity region corresponding to the Newport-Inglewood fault
- Results indicate that with large, dense, and long-duration seismic arrays, we can resolve high-resolution subsurface structures using ambient seismic noise data